Inorganic Chemistry

Article

pubs.acs.org/IC

B-Site Deficiencies in *A*-site-Ordered Perovskite $LaCu_3Pt_{3.75}O_{12}$

Mikiko Ochi,[†] Ikuya Yamada,*[,†,‡,§] Kenya Ohgushi,[∥] Yoshihiro Kusano,[⊥] Masaichiro Mizumaki,[⊗,○] Ryoji Takahashi,[†] Shunsuke Yagi,[‡] Norimasa Nishiyama,[#,§,Δ] Toru Inoue,[#] and Tetsuo Irifune[#]

[†]Department of Chemistry, Graduate School of Science and Engineering, Ehime University, 2-5 Bunkyo-cho, Matsuyama, Ehime 790-8577, Japan

[‡]Nanoscience and Nanotechnology Research Center, Osaka Prefecture University, 1-2 Gakuen-cho, Naka-ku, Sakai, Osaka 599-8570, Japan

[§]Precursory Research for Embryonic Science and Technology (PRESTO), Japan Science and Technology Agency (JST), Chiyoda-ku, Tokyo 102-0075, Japan

[∥]Institute for Solid State Physics (ISSP), University of Tokyo, 5-1-5 Kashiwanoha, Kashiwa, Chiba 227-8581, Japan

[⊥]Department of Applied Arts and Design, Kurashiki University of Science and the Arts, Kurashiki, Okayama 712-8505, Japan

[⊗]Japan Synchrotron Radiation Research Institute (JASRI), Sayo-cho, Sayo-gun, Hyogo 679-5198, Japan

[○]Core Research for Evolutional Science and Technology (CREST), Japan Science and Technology Agency (JST), 5 Sanbancho, Chiyoda-ku, Tokyo 102-0075, Japan

[#]Geodynamics Research Center (GRC), Ehime University, 2-5 Bunkyo-cho, Matsuyama, Ehime 790-8577, Japan

Supporting Information

ABSTRACT: An *A*-site-ordered perovskite $LaCu_3Pt_{3.75}O_{12}$ was synthesized by replacing Ca^{2+} with La^{3+} in a cubic quadruple $AA'_3B_4O_{12}$-type perovskite $CaCu_3Pt_4O_{12}$ under high-pressure and high-temperature of 15 GPa and 1100 °C. In $LaCu_3Pt_{3.75}O_{12}$, 1/16 of *B*-site cations are vacant to achieve charge balance. The *B*-site deficiencies were evidenced by crystal structure refinement using synchrotron X-ray powder diffraction, hard X-ray photoemission spectroscopy, and soft X-ray absorption spectroscopy, leading to the ionic model $La^{3+}Cu^{2+}{}_3Pt^{4+}{}_{3.75}O^{2-}{}_{12}$. Magnetic susceptibility data for this compound indicated a spin-glass-like behavior below T_g = 3.7 K, which is attributed to disturbance of the antiferromagnetic superexchange interaction by the *B*-site deficiencies.

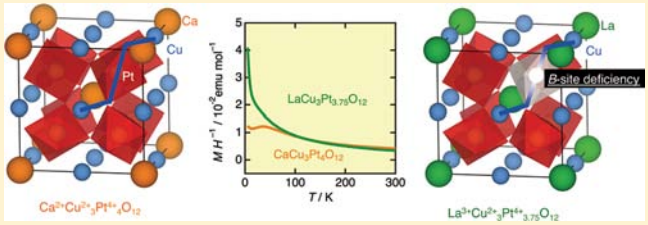

INTRODUCTION

Perovskite oxides ABO_3 have been investigated extensively because of their fascinating electronic properties. Cation substitutions of *A*/*B*-sites drastically change the structure and electronic properties of perovskite oxides, leading to intriguing phenomena such as metal−insulator transitions, colossal magnetoresistance, and superconductivity.[1] Large differences in ionic size, valence, and coordination preference between the substituting and substituted ions induce perovskite-type structures with cation ordering. $CaCu_3Ti_4O_{12}$ is a typical example of a quadruple *A*-site-ordered perovskite, $AA'_3B_4O_{12}$, with a unit cell of $2a_p \times 2a_p \times 2a_p$ (Figure 1a),[2,3] where a_p represents the unit cell edge of a simple ABO_3 perovskite. In this structure, *A*-sites of a simple perovskite are segregated into *A*- and *A*′-sites with 1:3-type ordering. Three quarters of *A*-sites (=*A*′-sites) are surrounded by four nearest-neighbor oxygen ions to form pseudosquare $A'O_4$ planes. The other quarter of *A*-sites are coordinated by 12 oxygen ions, forming AO_{12} icosahedra. Extensive research on this system has found a wide variety of interesting phenomena such as high dielectric constant,[4] low-field magnetoresistance,[5,6] heavy-fermion-like behavior,[7] and giant negative thermal expansion.[8]

$AA'_3B_4O_{12}$-type perovskites can tolerate various types of cation deficiencies. For example, $\square_1Cu^{2+}{}_3Ti^{4+}{}_2Ta^{5+}{}_2O^{2-}{}_{12}$ has a full vacancy at *A*-sites, and $\square_1(\square_1Cu^{2+}{}_2)Ta^{5+}{}_4O^{2-}{}_{12}$ contains full- and 1/3-vacancies at *A*- and *A*′-sites, respectively, where $\square$ represents a vacancy.[9] $Ln^{3+}{}_{2/3}\square_{1/3}Cu^{2+}{}_3Ti^{4+}{}_4O^{2-}{}_{12}$ (or $Ln_{2/3}Cu_3Ti_4O_{12}$, *Ln*: trivalent lanthanide metal ion) contains deficiencies at one-third of *A*-site.[9] In all of these compounds, cation deficiencies are introduced to achieve electrical neutrality. The effects of *A*-site deficiencies on the magnetic properties for $Ln_{2/3}Cu_3Ti_4O_{12}$ perovskites have been compared with those of the parent compound $CaCu_3Ti_4O_{12}$.[10] $CaCu_3Ti_4O_{12}$ is an antiferromagnetic insulator with a Néel temperature (T_N) of 25 K, in which long-range ordering of the localized Cu^{2+} spins (S = 1/2) are dominated by antiferromagnetic superexchange interaction via the Cu−O−Ti−O−Cu pathway, although weak direct ferromagnetic interaction works in Cu−Cu.[11] Because *A*-site ions are not involved in the magnetic interaction of *A*′-site Cu spins and the magnetic moments of *Ln* 4f electrons are decoupled to Cu 3d spins, the magnetic properties

Received: December 21, 2012
Published: March 21, 2013

   dx.doi.org/10.1021/ic302809v | *Inorg. Chem.* 2013, 52, 3985−3989

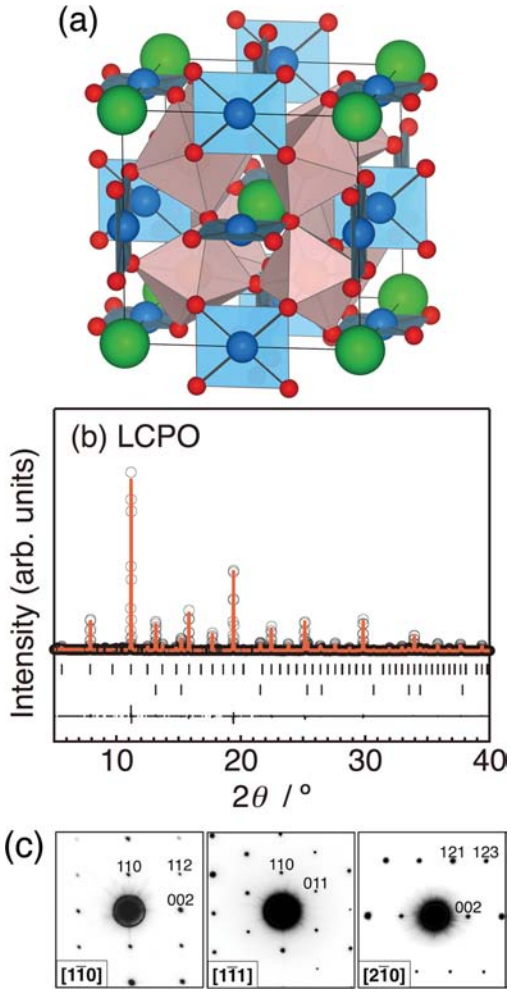

Figure 1. (a) Crystal structure of an $AA'_3B_4O_{12}$-type perovskite. Large green spheres, medium blue spheres with planar coordination, and small red spheres represent A, A', and O atoms, respectively. Octahedra represent BO_6 polyhedral units. (b) Observed SXRD pattern and the Rietveld refinement result for $LaCu_3Pt_{3.75}O_{12}$. Dotted and solid lines are observed and calculated patterns, respectively. The difference between the observed and the calculated patterns is shown at the bottom. The vertical marks indicate the Bragg peak positions of $LaCu_3Pt_{3.75}O_{12}$ (upper) and platinum metal (lower). (c) ED patterns for $LaCu_3Pt_{3.75}O_{12}$ along the [1$\bar{1}$0], [1$\bar{1}$1], and [2$\bar{1}$0] zone axes at 300 K.

of Cu ions are unchanged in $Ln_{2/3}Cu_3Ti_4O_{12}$ perovskites, resulting in almost the same Néel temperatures ($T_N \sim 25$ K) as $CaCu_3Ti_4O_{12}$.[10] Hence, A-site deficiencies hardly affect the magnetic properties of A'-site Cu spins.

Recently, we reported a platinum-based $AA'_3B_4O_{12}$-type perovskite $CaCu_3Pt_4O_{12}$ (CCPO).[12] Long-range antiferromagnetic ordering of the Cu spins in CCPO (T_N = 40 K) is dominated by superexchange interaction through the Cu−O−Pt−O−Cu pathway in the same manner as $CaCu_3Ti_4O_{12}$,[11] where Pt^{4+} ions in a low spin configuration ($5d^6$, $t_{2g}^6e_g^0$) are considered to play a role in the superexchange interaction like the Ti^{4+} ions ($3d^0$, $t_{2g}^0e_g^0$) of $CaCu_3Ti_4O_{12}$. In this paper, we report replacement of Ca^{2+} by La^{3+} in CCPO using high-pressure and high-temperature of 15 GPa and 1100 °C. Crystal structure refinement based on electron diffraction (ED), synchrotron X-ray powder diffraction (SXRD), hard X-ray photoemission spectroscopy (XPS), and soft X-ray absorption spectroscopy (XAS) revealed that the obtained sample contains cation deficiencies at B-sites, and can be represented as a nominal chemical formula of $LaCu_3Pt_{3.75}O_{12}$ (LCPO). This is the first example of B-site deficiencies in $AA'_3B_4O_{12}$-type perovskites. The deficiencies at the Pt sites realize charge balance to form the ionic state of $La^{3+}Cu^{2+}{}_3Pt^{4+}{}_{3.75}O^{2-}{}_{12}$. Magnetic susceptibility measurements indicate a spin-glass-like behavior below T_g = 3.7 K, in contrast to the long-range antiferromagnetic ordering for CCPO below 40 K.

EXPERIMENTAL SECTION

A polycrystalline LCPO sample was synthesized from a mixture of La_2O_3, CuO, Cu_2O, and PtO_2, all 99.9% and purchased from Rare Metallic, Japan, in a molar ratio of 1:4:1:8. The La_2O_3 powder was calcined at 1000 °C for 24 h before use. The starting mixture was added to a gold capsule with an inner diameter of 2.8 mm and a height of 5.0 mm in a nitrogen-filled glovebox. The gold capsule was placed into an octahedral (Mg,Co)O pressure transmitting medium with a graphite furnace. The (Mg,Co)O medium was surrounded by eight WC anvils with truncation and compressed to 15 GPa using a Kawai-type high-pressure apparatus at GRC, Ehime University. The sample was heated up to 1100 °C in 20 min, kept at this temperature for 5 min, and then the pressure was released. A reference polycrystalline CCPO sample was prepared using the procedure described in the literature.[12] SXRD data were acquired using a Debye−Scherrer camera at the BL02B2 beamline of SPring-8. The wavelength was determined to be 0.51852 Å using a CeO_2 standard. The SXRD data was refined using the Rietveld program RIETAN-FP.[13] ED patterns were collected at room temperature using a transmission electron microscope (TEM, TOPCON EM-002B) with an accelerating voltage of 200 kV. XPS measurements were conducted with a spectrometer (VG-SCIENTA R-4000) installed at the BL47XU beamline of SPring-8. The incident photon energy was 7.94 keV. The XPS data of the inner-shell electrons of Pt 4d were collected at 300 K. The energy scale was calibrated using the Fermi edge of a gold-deposited sample. The energy resolution of this system was about 280 meV around 7.94 keV. XAS measurements were performed using the total electron yield method at the BL27SU beamline of SPring-8. The Cu $L_{2,3}$-edge XAS spectra were collected at 300 K. The energy resolution, $\Delta E/E$, was greater than 5000. Magnetic susceptibility data were collected between 5 and 300 K in an external field of 1000 Oe, and between 2 and 5 K in an external field of 50 Oe, in zero-field-cooling (ZFC) and field-cooling (FC) modes using a SQUID magnetometer (Quantum Design, MPMS-XL).

RESULTS AND DISCUSSION

SXRD data and the results of the Rietveld refinement of LCPO are presented in Figure 1b. The primary phase was identified as a cubic $AA'_3B_4O_{12}$-type perovskite with a lattice constant a of ~7.54 Å. The sample contained metallic platinum (13.5 wt %) and unknown phase(s) (estimated to be a few wt % at most) as impurities. ED patterns of LCPO along the [1$\bar{1}$0], [1$\bar{1}$1], and [2$\bar{1}$0] zone axes are shown in Figure 1c. These ED patterns could be indexed with a space group $Im\bar{3}$ (No. 204). The initial crystal structure refinement for LCPO was performed using a stoichiometric model $LaCu_3Pt_4O_{12}$, which is isostructural with CCPO.[12] The structure model for the final refinement was considered based on the spectroscopic data, as discussed later.

The valence states of Pt and Cu ions in CCPO and LCPO were investigated using XPS and XAS. Figure 2a shows Pt 4d XPS data of CCPO and LCPO. The binding energy of Pt $4d_{5/2}$ of CCPO is about 317.6 eV, which is close to that of $Pt^{4+}O_2$ (~318 eV).[14] XAS spectra of the Cu $L_{2,3}$-edges of CCPO and LCPO are depicted in Figure 2b. The spectral shapes and peak positions (930.3 and 950.6 eV for L_3- and L_2-edges, respectively) of CCPO are similar to those of $Ca^{2+}Cu^{2+}{}_3Ti^{4+}{}_4O^{2-}{}_{12}$ (~930 and ~950 eV).[15] The above XPS

dx.doi.org/10.1021/ic302809v | Inorg. Chem. 2013, 52, 3985−3989

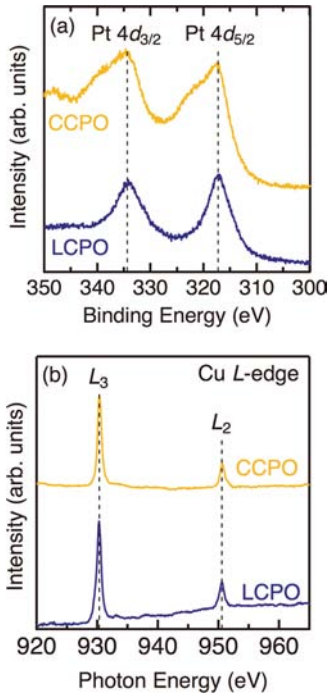

Figure 2. (a) Pt 4d XPS spectra of $LaCu_3Pt_{3.75}O_{12}$ and $CaCu_3Pt_4O_{12}$ at room temperature. (b) XAS of Cu *L*-edges of $LaCu_3Pt_{3.75}O_{12}$ and $CaCu_3Pt_4O_{12}$ at room temperature.

and XAS data confirm that the valence states of Pt and Cu ions are +4 and +2, respectively, and agree with the ionic model $Ca^{2+}Cu^{2+}{}_3Pt^{4+}{}_4O^{2-}{}_{12}$ as suggested by the structure refinement in our previous report.[12] The binding energy of Pt $4d_{5/2}$ XPS and peak positions of Cu $L_{2,3}$-edge XAS data of LCPO are close to those of CCPO (Figure 2a and b, respectively). Therefore, the valence states of Pt and Cu ions in LCPO are identical to those in CCPO, and the valences of these two ions are not changed by substitution of La^{3+} for Ca^{2+}. The above spectroscopic analyses clearly exclude the stoichiometry of the LCPO sample because reduced ions of either $Pt^{3.75+}$ or $Cu^{1.67+}$ should be generated to maintain the charge balance of the stoichiometric composition of $LaCu_3Pt_4O_{12}$.

We considered possible structure models for LCPO to explain its spectroscopic data. Cation deficiencies at La, Cu, or Pt sites can rationally explain the Cu^{2+} and Pt^{4+} valence states, with corresponding structure models $La^{3+}{}_{2/3}Cu^{2+}{}_3Pt^{4+}{}_4O^{2-}{}_{12}$, $La^{3+}Cu^{2+}{}_{2.5}Pt^{4+}{}_4O^{2-}{}_{12}$, and $La^{3+}Cu^{2+}{}_3Pt^{4+}{}_{3.75}O^{2-}{}_{12}$, respectively. To reveal the most plausible model, we refined the occupancy factor *g* for each site using these models. The *g* values obtained from the refinement were 1.101(6), 1.077(7), and 0.933(4) for La, Cu, and Pt sites, respectively. In the case of the former two models, the *g* values are meaningless because they are larger than unity, implying there are no deficiencies at La and Cu sites. In contrast, refinement of the latter model with deficiencies at Pt sites gave a plausible *g* value. The nominal chemical formula calculated from the final refinement result for this model was $LaCu_3Pt_{3.732(16)}O_{12}$, which is identical to that of the *B*-site deficiency model $LaCu_3Pt_{3.75}O_{12}$ within the analytical error. The reliability factors of the final refinement (R_{wp} = 7.377%, R_B = 2.901%, and goodness-of-fit, GOF = 1.2430) were improved from those based on the stoichiometric composition model (R_{wp} = 7.754%, R_B = 3.036%, and GOF = 1.3063). The *B*-site deficiencies are uncommon in perovskite-type compounds. However, since ~8% *B*-site deficiencies were confirmed in a simple perovskite,[16] 1/16 (= 6.25%) in LCPO may be tolerated. Therefore, we conclude that the LCPO phase obtained in this study is $LaCu_3Pt_{3.75}O_{12}$. The absence of superlattice reflections in the ED patterns suggests that the deficiencies at Pt sites are randomly distributed. The structure parameters and selected metal−oxygen bond lengths of LCPO are listed in Table 1. The bond valence sums (BVS)[17,18] for La, Cu, and Pt were 3.15, 2.05, and 3.99, respectively, which are consistent with the above-mentioned ionic model.

Table 1. Refined Structure Parameters, Selected Bond Lengths, and BVS for $LaCu_3Pt_{3.75}O_{12}$[a]

g (Pt)	0.933(4)
x (O)	0.3099(10)
y (O)	0.1704(11)
B (La)/Å^2	0.57(5)
B (Cu)/Å^2	0.65(5)
B (Pt)/Å^2	0.477(13)
B (O)/Å^2	1.47(18)
La−O (×12)/Å	2.667(9)
Cu−O (×4)/Å	1.925(7)
Cu−O (×4)/Å	2.869(9)
Pt−O (×6)/Å	2.030(3)
BVS (La)	3.15
BVS (Cu)	2.05
BVS (Pt)	3.99

[a]Space group: $Im\bar{3}$ (No.204); atomic sites: La 2*a* (0, 0, 0), Cu 6*b* (0, $^1/_2$, $^1/_2$), Pt 8*c* ($^1/_4$, $^1/_4$, $^1/_4$), O 24*g* (*x*, *y*, 0); lattice constant *a* = 7.54045(10) Å, R_{wp} = 7.377%, R_B = 2.901%, and GOF = 1.2430. The site occupancy factors *g* for La, Cu, and O were fixed at unity.

The physical properties of LCPO were investigated to elucidate the effect of *B*-site deficiencies. Both LCPO and CCPO exhibited high resistivity (>~10^6 Ω cm at room temperature), which disturbed electrical resistivity measurement and indicated their insulating nature. These compounds are expected to be band insulators with no effective conduction carriers, as expected from the low spin configuration ($5d^6$, $t_{2g}{}^6e_g{}^0$) of the Pt^{4+} ions in the octahedral coordination of *B*-sites. The magnetic properties of LCPO differed drastically from the antiferromagnetic behavior of CCPO. Figure 3a shows the temperature dependence of the magnetic susceptibility of LCPO between 5 and 300 K in the ZFC mode. The FC data (not shown) were almost identical to those in the ZFC mode in this temperature range. The inverse magnetic susceptibility follows the Curie−Weiss law down to 15 K (Figure 3b). Note that the antiferromagnetic transition disappears in LCPO. LCPO exhibits spin-glass-like behavior below 3.7 K (the inset of Figure 3a), as evidenced by a deviation between FC and ZFC modes. The inverse magnetic susceptibility, $\chi^{-1}(T)$ (= H/M), of LCPO in the temperature range 100−300 K were fitted using the Curie−Weiss formula: $\chi^{-1}(T) = (T - \theta)/C$, where *C* and θ are the Curie constant and Weiss temperature, respectively. Curie−Weiss fitting gave *C* = 1.188(5) emu K/mol and θ = −33.2(2) K. The effective paramagnetic moment of LCPO is calculated to be 1.78 μ_B per Cu, which is consistent with the theoretical value of 1.75 μ_B for Cu^{2+} ions (*S* = 1/2).

The above experimental results demonstrate that the LCPO sample prepared under high-pressure and high-temperature of 15 GPa and 1100 °C contains a number of cation deficiencies at *B*-sites and that the valence states of the Cu^{2+} and Pt^{4+} ions are retained. The magnetic properties changed from the long-

dx.doi.org/10.1021/ic302809v | Inorg. Chem. 2013, 52, 3985−3989

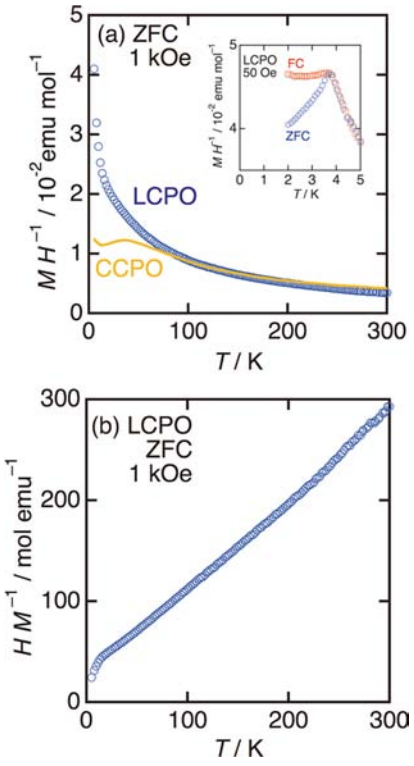

Figure 3. (a) Temperature dependence of the magnetic susceptibility in ZFC mode for $LaCu_3Pt_{3.75}O_{12}$ and $CaCu_3Pt_4O_{12}$ (data from ref 12) in an external field of 1000 Oe between 5 and 300 K. The inset shows the temperature dependence of the magnetic susceptibility in ZFC and FC modes in an external field of 50 Oe between 2 and 5 K. (b) Inverse magnetic susceptibility in ZFC mode for $LaCu_3Pt_{3.75}O_{12}$ in an external field of 1000 Oe between 5 and 300 K.

range antiferromagnetic ordering of Cu spins for CCPO to short-range spin-glass-like ordering for LCPO. Cation deficiencies at *B*-sites in $AA'_3B_4O_{12}$-type perovskites have not been reported to date, whereas cation deficiencies at *A*- and *A*′-sites to maintain electric neutrality have.[9] In the case of LCPO, the robust valence state of Pt^{4+} does not tolerate electron-doping introduced by substitution of La^{3+} for Ca^{2+}, so *B*-site cation deficiencies maintain the electric neutrality of this compound. It is interesting that deficiencies at different crystallographic sites (*A*-, *A*′-, or *B*-sites) play a similar role in keeping the charge balance of $AA'_3B_4O_{12}$-type perovskites. The factor determining the deficient sites is not clear at this stage, but our attempts to prepare *A*-site-deficient $La^{3+}{}_{2/3}Cu^{2+}{}_3Pt^{4+}{}_4O^{2-}{}_{12}$ and *B*-site-deficient $La^{3+}Cu^{2+}{}_3Ti^{4+}{}_{3.75}O^{2-}{}_{12}$ failed using high pressures of up to 15 GPa. Therefore, the preference for deficient sites may be unique for each compound.

The probable origin of the short-range spin-glass-like magnetic ordering of Cu spins in LCPO can be attributed to *B*-site deficiencies. In CCPO, two kinds of magnetic exchange interactions are proposed; one is an antiferromagnetic superexchange interaction via the Cu−O−Pt−O−Cu pathway and the other is a direct ferromagnetic interaction between nearest-neighboring Cu ions.[12] The antiferromagnetic nature of CCPO indicates that the former interaction dominates the latter in this compound. However, in the case of LCPO, the antiferromagnetic superexchange interaction seems to be randomly disturbed by the *B*-site deficiencies because magnetic exhange interaction does not likely work in the Cu−O−□−O−Cu pathway. Thus, the magnetic interactions in LCPO should provide magnetically disordered states, resulting in the short-range spin-glass-like magnetic ordering. This is in contrast to the small influence that *A*-site deficiencies have on the magnetic properties of $Ln_{2/3}Cu_3Ti_4O_{12}$ perovskites,[10] confirming that the Pt ions at *B*-sites contribute substantially to the magnetic properties of LCPO.

In conclusion, we synthesized the *A*-site-ordered perovskite $LaCu_3Pt_{3.75}O_{12}$ under high pressure and high temperature of 15 GPa and 1100 °C. *B*-site deficiencies with a proportion of 1/16 were evidenced by the Rietveld refinement of a structure model derived from electron diffraction, X-ray photoemission, and X-ray absorption spectroscopy. The spin-glass-like magnetic properties of LCPO are explained by random disturbance of the antiferromagnetic superexchange interaction caused by the *B*-site cation deficiencies.

■ ASSOCIATED CONTENT

Ⓢ Supporting Information

Crystallographic data for $LaCu_3Pt_{3.75}O_{12}$ (CIF). This material is available free of charge via the Internet at http://pubs.acs.org.

■ AUTHOR INFORMATION

Corresponding Author

*E-mail: i-yamada@21c.osakafu-u.ac.jp. Phone: +81-72-254-9817.

Present Address

[Δ]Deutsches Elektronen Synchrotron (DESY), 22607 Hamburg, Germany.

Notes

The authors declare no competing financial interest.

■ ACKNOWLEDGMENTS

Synchrotron radiation experiments were performed at SPring-8 with the approval of the Japan Synchrotron Radiation Research Institute (Proposal Nos. 2010B1707, 2011B1009, 2011B1094, and 2012A1660). Magnetic susceptibility measurements were performed at the Institute for Solid State Physics, University of Tokyo. This work was partly supported by JST-TRIP.

■ REFERENCES

(1) Imada, M.; Fujimori, A.; Tokura, Y. *Rev. Mod. Phys.* **1998**, *70*, 1039−1263.
(2) Deschanvres, A.; Raveau, B.; Tollermer, M. *Bull. Soc. Chim. Fr.* **1967**, *11*, 4077−4078.
(3) The crystal structure is drawn by using VESTA. Momma, K.; Izumi, F. *J. Appl. Crystallogr.* **2008**, *41*, 653−658.
(4) Subramanian, M. A.; Sleight, A. W. *Solid State Sci.* **2002**, *4*, 347−351.
(5) Zeng, Z.; Greenblatt, M.; Subramanian, M. A.; Croft, M. *Phys. Rev. Lett.* **1999**, *82*, 3164−3167.
(6) Alonso, J. A.; Sanchez-Benitez, J.; De Andres, A.; Martinez-Lope, M. J.; Casais, M. T.; Martinez, J. L. *Appl. Phys. Lett.* **2003**, *83*, 2623−2625.
(7) Kobayashi, W.; Terasaki, I.; Takeya, J.; Tsukada, I.; Ando, Y. *J. Phys. Soc. Jpn.* **2004**, *73*, 2373−2376.
(8) Yamada, I.; Tsuchida, K.; Ohgushi, K.; Hayashi, N.; Kim, J.; Tsuji, N.; Takahashi, R.; Matsushita, M.; Nishiyama, N.; Inoue, T.; Irifune, T.; Kato, K.; Takata, M.; Takano, M. *Angew. Chem., Int. Ed.* **2011**, *50*, 6579−6582.
(9) Bochu, B.; Deschizeaux, M. N.; Joubert, J. C.; Collomb, A.; Chenavas, J.; Marezio, M. *J. Solid State Chem.* **1979**, *29*, 291−298.

(10) Dittl, A.; Krohns, S.; Sebald, J.; Schrettle, F.; Hemmida, M.; von Nidda, H. A. K.; Riegg, S.; Reller, A.; Ebbinghaus, S. G.; Loidl, A. *Eur. Phys. J. B* **2011**, *79*, 391−400.
(11) Mizumaki, M.; Saito, T.; Shiraki, H.; Shimakawa, Y. *Inorg. Chem.* **2009**, *48*, 3499−3501.
(12) Yamada, I.; Takahashi, Y.; Ohgushi, K.; Nishiyama, N.; Takahashi, R.; Wada, K.; Kunimoto, T.; Ohfuji, H.; Kojima, Y.; Inoue, T.; Irifune, T. *Inorg. Chem.* **2010**, *49*, 6778−6780.
(13) Izumi, F.; Momma, K. *Solid State Phenom.* **2007**, *130*, 15−20.
(14) Escard, J.; Pontvianne, B.; Chenebaux, M. T.; Cosyns. *J. Bull. Soc. Chim. France* **1975**, *11*, 2400−2408.
(15) McGuinness, C.; Downes, J. E.; Sheridan, P.; Glans, P. A.; Smith, K. E.; Si, W.; Johnson, P. D. *Phys. Rev. B* **2005**, *71*, 195111.
(16) Ji, D. H.; Tang, G. D.; Li, Z. Z.; Han, Q. J.; Hou, X.; Bian, R. R.; Liu, S. R. *Appl. Phys. Lett.* **2012**, *111*, 113902.
(17) Brown, I. D.; Altermatt, D. *Acta Crystallogr.* **1985**, *B41*, 244−247.
(18) The BVS were calculated using the following parameters: b_0 = 0.37 for all atoms, r_0 = 2.172 for La^{3+}, r_0 = 1.649 for Cu^{2+}, and r_0 = 1.879 for Pt^{4+}.